GATING AND PERMEATION PROPERTIES OF TWO TYPES OF CALCIUM CHANNELS IN NEUROBLASTOMA CELLS

MITSUNOBU YOSHII, AKINOBU TSUNOO, AND TOSHIO NARAHASHI

Department of Pharmacology, Northwestern University Medical School, Chicago, Illinois 60611

ABSTRACT The gating and permeation properties of two types of calcium channels were studied in the neuroblastoma cell line N1E-115. Calcium channel currents as carried by Ba^{2+} (50 mM) were recorded using the whole-cell variation of the patch electrode voltage-clamp technique. The two types of calcium channels showed similar membrane potential dependence with respect to the steady-state activation and inactivation gating properties. However, the properties of the long-lasting type II channels were shifted ~30 mV in the depolarizing direction compared with those of the transient type I channels. Activation of type I channels developed with a sigmoidal time course which was described by m^2 kinetics, whereas the activation of type II channels was described by a single exponential function. Tail current upon repolarization followed an exponential decay in either type of calcium channels. In comparison to type I channels, the activation process of type II channels was shifted ~30 mV in the positive direction, while the deactivation process showed a 60 mV shift in the positive direction. The rate constants of activation obtained from the activation and deactivation processes indicated that under comparable membrane potential conditions, type II channels close 2.4 times faster than type I channels upon repolarization. When external 50 mM Ba^{2+} was replaced with Ca^{2+} or Sr^{2+} on the equimolar basis, the amplitudes of transient and long-lasting currents were altered without a significant change in their time courses. The ion permeability ratios determined from the maximum amplitude of the inward current were as follows: Ba^{2+} (1.0) = Sr^{2+} (1.0) > Ca^{2+} (0.7) for type I channels, and Ba^{2+} (1.0) > Sr^{2+} (0.7) > Ca^{2+} (0.3) for type II channels. Replacement of Ba^{2+} with Ca^{2+} caused a 10–12 mV positive shift in the current-voltage relation for type II channels. However, the shift for type I channels was much less. This suggests that negative surface charges are present around type II channels. After correction for the surface charge effect on the ion permeation, there was no significant difference between the permeability ratios of these cations for the two channel types. It was concluded that the two types of calcium channels have many common properties in their gating and permeation mechanisms despite their differential voltage sensitivity and ion selectivity.

INTRODUCTION

It has been suggested that cultured neuroblastoma cells (N1E-115) are endowed with two types of voltage-sensitive calcium channels (Fishman and Spector, 1981; Tsunoo et al., 1984). In a preceding paper (Narahashi et al., 1987), it was shown that the inward Ba^{2+} current through calcium channels was separated into two components, i.e., a transient and a long-lasting current. The calcium channel responsible for the transient current was referred to as "type I" channel, and the calcium channel responsible for the long-lasting current was referred to as "type II" channel. The type II channel showed a much higher sensitivity to the calcium channel blocker Cd^{2+} than the type I channel. The type II channel activity was enhanced selectively by an elevation of the intracellular level of cyclic AMP. Type II channel currents were selectively blocked by leucine-enkephalin (Tsunoo et al., 1986). These results are in favor of the idea that the two types of channels are different entities rather than one channel exhibiting two different modes. However, it remains to be seen whether the gating and ion permeation mechanisms are different between the two types of calcium channels.

We have analyzed the gating and ion permeation mechanisms of the two types of calcium channels using cultured neuroblastoma cells. It was found that a variety of potential-dependent kinetic parameters of type II channels was shifted ~30 mV in the direction of more positive potential from that of type I channels. However, the deactivation (or turn-off) process of type II channels was much faster than that of type I channels even if the 30 mV shift was taken into account. The permeability to Ca^{2+}, Sr^{2+}, and Ba^{2+} appeared to be somewhat different between the two channel types, but the difference disappeared after correction for the surface charge effect. Preliminary results of these experiments have been reported elsewhere (Yoshii et al., 1985).

METHODS

The methods were essentially the same as those described previously (Narahashi et al., 1987). Mouse neuroblastoma cells (N1E-115) were

M. Yoshii's and A. Tsunoo's present address is Meiji Institute of Health Science, 540 Naruda, Odawara, Kanagawa 250, Japan.
Address correspondence to Toshio Narahashi.

cultured and differentiated into mature nerve cells (Kimhi et al., 1976; Moolenaar and Spector, 1978; Quandt and Narahashi, 1984). 3–7 d before use, cells were plated on glass coverslips, and 2% DMSO was added to the culture medium (90% DME + 10% new-born calf serum) to facilitate cell differentiation.

A whole-cell patch-clamp technique (Hamill et al., 1981) was used to record ionic currents under voltage-clamp conditions. To improve space-clamp conditions, cells with processes exceeding the cell diameter were never used. A suction pipette with a resistance of 0.8–2.0 MΩ was placed onto the cell surface, and the membrane under the pipette tip was ruptured by applying gentle suction to the pipette. The potential inside the cell was controlled at the ground level. An inverted command voltage was applied to the external solution via a bath electrode. Currents through the pipette in response to the command voltages were recorded by a current-to-voltage converter which was directly connected to the suction pipette. A part of the output voltage of the current recording was added to the command voltage to compensate for the series resistance. Data were recorded and analyzed with a digital oscilloscope (model 2090-3C; Nicolet Instrument Corp., Fremond, CA) and its associated disk drive, and the results were traced on an X-Y plotter (model 7040A; Hewlett-Packard Co., Palo Alto, CA). Unless otherwise noted, linear leakage components determined at membrane potentials ranging between −120 and −60 mV have been subtracted from the records shown in this paper.

The external and internal (pipette-filling) solutions were designed to separate calcium channel currents from other potential-dependent currents. A high Ba^{2+} (50 mM) solution was used as the standard external solution to enhance the current amplitude. To suppress the outward K^+ current, 25 mM tetraethylammonium (TEA) was added to the external media (Hille, 1967) and K^+ was replaced with Cs^+ in both external and internal solutions. Sodium channels were always blocked by 0.5 μM-tetrodotoxin (TTX) (Narahashi et al., 1964; Quandt and Narahashi, 1984). The standard external solution contained (in mM): BaCl$_2$, 50; NaCl, 30; CsCl, 5; glucose, 25; TEA-Cl, 25; and TTX, 0.5 μM. The pH was adjusted to 7.3–7.4 with 5 mM Hepes-Cs. The internal solution contained (in mM): Cs-glutamate, 130; MgCl$_2$, 2.5; and glucose, 5. The pH of the internal solution was adjusted to 7.0–7.1 with 10 mM Pipes-Na (the Na$^+$ concentration is calculated to be ~16 mM).

Unless otherwise stated, experiments were carried out at room temperature (22°–23°C). The bath temperature was recorded with a small thermocouple probe, which was placed adjacent to the cell being examined.

RESULTS

I. Gating Properties

Steady-state Activation. Current-voltage (I-V) relations for the peak amplitude of the transient current through type I calcium channels are illustrated in Fig. 1 *A*. The current was isolated from that through type II channels in the manner described before (Narahashi et al., 1987). In short, the type II current measured at the end of the 160-ms depolarization pulse was subtracted from the peak inward current to isolate the type I current. The current was generated at −50 mV, increased its amplitude with further depolarization attaining a maximum at −20 mV. With depolarizations beyond −20 mV, the current amplitude decreased and approached zero at +60 mV. The steady-state currents through type II calcium channels were measured 160 ms after the onset of depolarizing pulse, and the I-V relationship is illustrated in Fig. 1 *B* (*solid circles*). As described previously (Narahashi et al., 1987), the current was contaminated with an outward current at potentials more positive than +20 mV. The

steady-state activation occurred at −20 mV and reached a maximum at potentials more positive than +10 mV. These results indicated that the potential dependence of the steady-state activation of type II channels was shifted 30 mV in the positive direction from that of type I channels.

The I-V relation for type I channels as shown in Fig. 1 *A* is nonlinear at the positive potential region and the reversal potential cannot be determined. Therefore, the constant field theory (Goldman, 1943; Hodgkin and Katz, 1949) was used to predict the maximum current amplitude of type I channels at its full activation (Ohmori and Yoshii, 1977; also see Hagiwara and Byerly, 1981). The solid curve in Fig. 1 *A* was calculated according to the constant field equation for a divalent cation so as to fit the data at large positive potentials at which the channels were expected to be fully activated. The ratio of the observed current amplitude to the theoretical curve yielded a steady-state activation level for a given potential. The results are shown in Fig. 2 *A* (*solid squares*).

For type II calcium channels, the method of curve-fitting as described in the preceding paragraph could not be used because of contamination by outward currents at large positive potentials. As an alternative method, the instantaneous current upon repolarization after the appearance of the long-lasting current was measured (Fig. 1 *B*, *crosses*). The amplitude of the instantaneous current upon repolarization to a fixed potential is a measure of the channel activity at the end of a depolarizing test pulse. The holding potential was reduced to −30 mV to inactivate type I channels. The duration of the test pulse was made as short as 50 ms to prevent development of the outward current, but it was long enough to achieve a steady-state activation. The repolarization potential was selected at −30 mV, at which the deactivation time course of the tail current was expressed by a single exponential function so that the initial amplitude of the instantaneous current was easily determined by extrapolating the falling phase to the zero time. The amplitude of the instantaneous current gave a relative level of the steady-state activation of the type II channel, and the results are shown in Fig. 2 *A* (*open squares*).

The steady-state activation curves for type I and type II calcium channels are similar in shape but different in midpoint potential: −20 mV for type I and +12 mV for type II with a difference of 32 mV. The slope factors for an *e*-fold change in the steady-state activation measured at the midpoint potentials were only slightly different between the two types of channels, 11 mV for type I channels and 12.5 mV for type II channels. The data indicated that the potential dependence of the steady-state activation of type II channels was shifted ~30 mV in the positive direction in parallel with that of type I channels.

The slightly steeper activation curve for type I channels as compared with that for type II channels may be explained as follows: The peak amplitude of type I current is dependent on both activation and inactivation gating
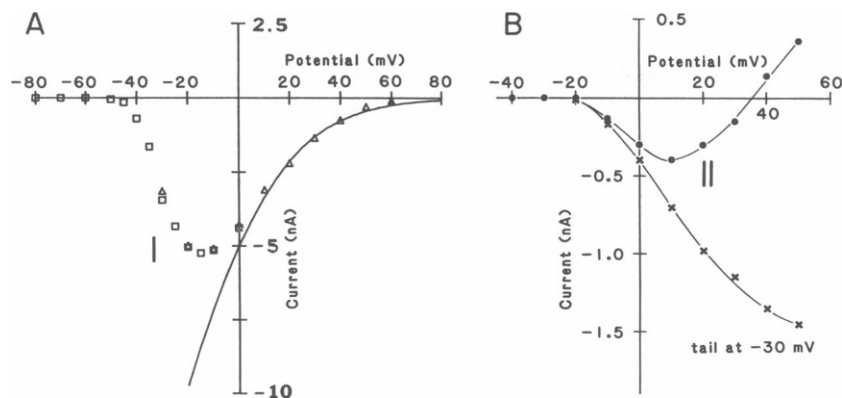
FIGURE 1 Current-voltage relations for transient (type I) and long-lasting (type II) Ba^{2+} currents through calcium channels of neuroblastoma cell membranes under voltage-clamp conditions. Leakage currents have been subtracted. External solution contained 50 mM Ba^{2+}, 0.5 μM TTX, and 25 mM TEA. (A) The peak amplitude of the transient current as separated from the long-lasting current by the conditioning depolarizing method described previously (Narahashi et al., 1987). Holding potential, -80 mV. Data from the same cell as that in Fig. 3 C in Narahashi et al. (1987). Triangles represent transient currents isolated by subtraction of long-lasting components that remained with a 5 s prepulse to -30 mV. Squares represent transient currents without the subtraction procedure. The solid curve is drawn according to the constant field equation for divalent cation: $I_{Ba} = (4F^2E_m/RT) \cdot P_{Ba}[Ba^{2+}]_0/[1 - \exp(2FE_m/RT)] = CE_m/[1 - \exp(E_m/13.18 \text{ mV})]$. C (constant) = 0.38 nA/mV. Temperature, 33.1°C. Cell, number 6. (B) The amplitude of the long-lasting current at the end of the 160-ms voltage pulse (●) and the instantaneous current at the beginning of a repolarization to -30 mV (×). Holding potential, -30 mV. The amplitude of the instantaneous current was determined by extrapolation to the zero-time on the assumption that the tail current decayed with a single exponential function. Room temperature. Cell, number 28.

kinetics. The peak current amplitude would be proportional to the theoretical maximum current amplitude at each membrane potential if the activation and inactivation kinetics had the same potential dependence. However, the τ_m curve is less steep than the τ_h curve at potentials from -50 to -30 mV, and steeper at potentials more positive than -30 mV. This may result in an under-estimation of the steady-state activation curve at potentials from -50 to -30 mV and an over-estimation at potentials more positive than -30 mV. Thus the observed difference in the slope of activation curve between the two channels may reflect this error.

Steady-state Inactivation. The transient calcium channel current was reduced in amplitude as the holding potential was made less negative. By analogy of the steady-state inactivation of sodium channels (Hodgkin and Huxley, 1952), the potential dependence of the calcium channel inactivation was described in the form of the h_∞ (Okamoto et al., 1976; Moolenaar and Spector, 1978). There is evidence that type II channels, although lacking in fast inactivation, show a slow inactivation (Fedulova et al., 1985). The steady-state inactivation of calcium channels was compared between the two types.

A test depolarizing pulse was preceded by a long-lasting (10 s) conditioning depolarization to various potentials. For type I channels, the test pulse was selected at -20 mV to observe a maximal current without contamination of the type II component (Narahashi et al., 1987). The relative amplitude of the current plotted against the membrane potential of the conditioning pulse yielded a steady-state inactivation curve for type I channels as shown in Fig. 2 B (*solid squares*). Inactivaiton was completely removed at potentials more negative than -70 mV, and became complete at potentials more positive than -30 mV. The half-inactivation potential was -51.5 mV, being very close

to the critical activation level of -50 mV. The slope factor was 4.0 mV with an e-fold change in inactivation. The results were in agreement with those obtained previously in the same preparation but for a different charge carrier of Ca^{2+} (Moolenaar and Spector, 1978).

To obtain a steady-state inactivation curve for type II channels, a test pulse to $+10$ mV, preceded by a 10-s conditioning depolarization to various potentials, was applied to induce a maximal long-lasting type II current. When the conditioning pulse was more negative than -30 mV, the current associated with a test pulse was contaminated by the type I current that had not been fully inactivated. The magnitude of the type II steady-state current was measured 160 ms after the onset of the test pulse as described previously (Narahashi et al., 1987). The conditioning depolarizing pulses to potentials more positive than -30 mV inactivated the type I component, generating the type II component alone. The relative amplitude of the type II current plotted against the membrane potential yielded a steady-state inactivation curve as shown in Fig. 2 B (*open squares*). Complete inactivation could not be obtained because the membrane was deteriorated at large, prolonged depolarization. A similar problem has been reported for the study of type II channels in the dorsal root ganglion cell (Fedulova et al., 1985). Nevertheless, the data clearly indicated that type II channels underwent steady-state inactivation in a manner similar to type I channels: half-inactivation occurred at -23 mV, a potential close to the critical activation level of -20 mV for type II channels. The difference between the midpoints of the two types of channels was 28.5 mV. The slope factor for type II channels was 5.0 mV for an e-fold change in inactivation, and was similar to that of type I channels.

Thus the potential dependence of the steady-state inactivation of type II calcium channels was shifted approximately 30 mV in the positive direction in parallel with that

A

Steady-state activation

1.0

0.5

0

30 mV

I   II

-80   -40   0   40

Potential (mV)

B

Steady-state inactivation

1.0

0.5

0

30 mV

I   II

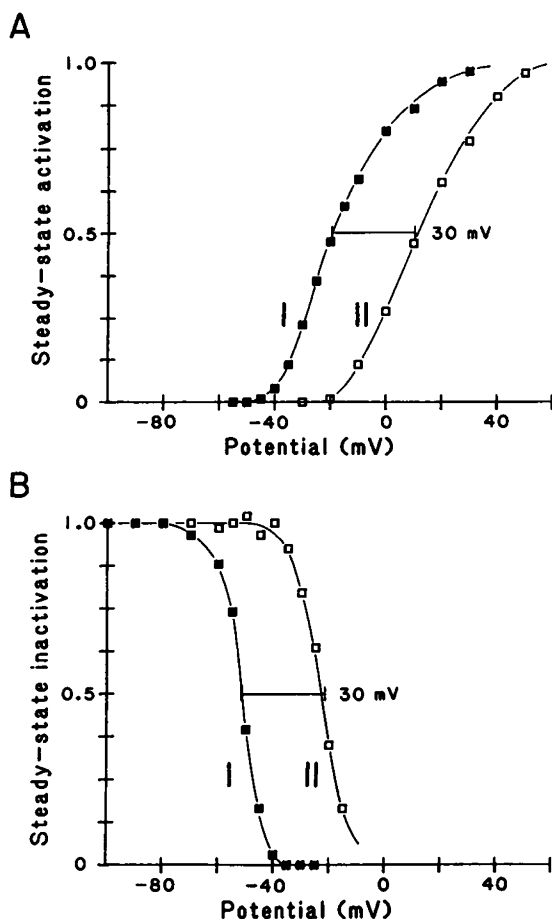-80   -40   0   40

Potential (mV)

FIGURE 2 Steady-state activation (A) and steady-state inactivation (B) of type I (■) and type II (□) calcium channels. (A) For type I channels, the ratio of the current amplitude to the maximum value predicted by the constant field theory is plotted against the membrane potential. For type II channels, relative amplitude of the instantaneous current associated with step repolarization is plotted against the membrane potential. The same data as those in Fig. 1. Solid curves are drawn by eye. (B) Relative amplitudes of the two types of currents plotted as a function of the membrane potential of the 10-s conditioning pulse. Test pulse: −20 mV for type I, +10 mV for type II. Solid curves are drawn by eye. Temperature: 33.1°C for type I and 34°C for type II. Cells: number 6 for type 1 and number 5 for type II.

of type I channels. There was no other difference in the steady-state gating properties between the two types of calcium channels.
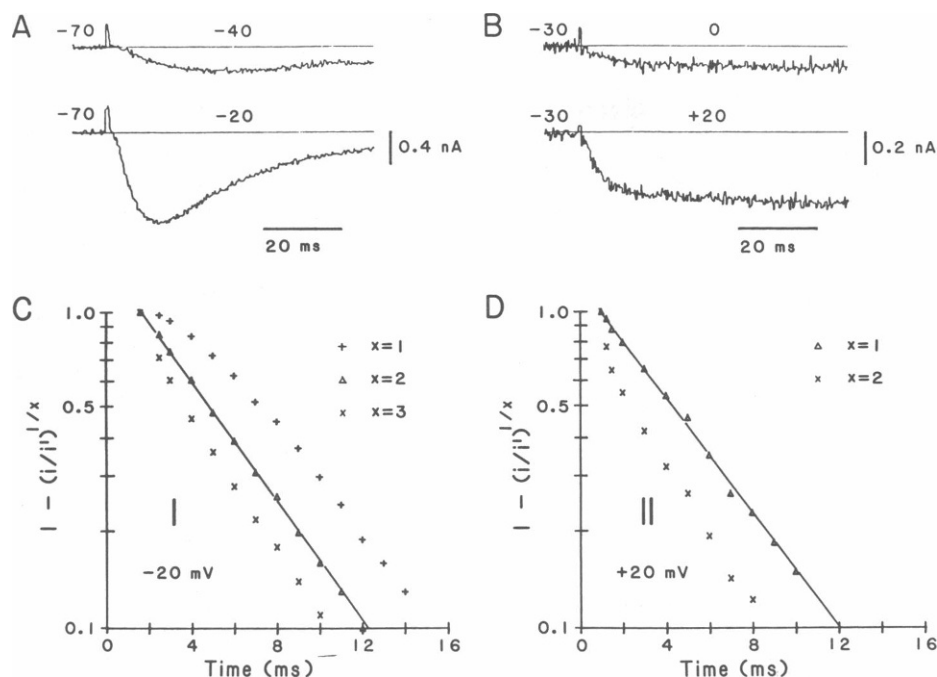
Time Course of Activation. Calcium channels in a variety of preparations are activated with a sigmoidal time course after a step depolarization (see Hagiwara and Byerly, 1981; Tsien, 1983). This was also the case for type I calcium channels in neuroblastoma cells (Quandt and Narahashi, 1984). However, in many earlier studies, a single exponential rise of calcium currents was observed (e.g., Okamoto et al., 1976). This difference has been attributed to the following two factors: (a) Recent improvement of voltage-clamp techniques allowed us to resolve an initial delay in the rising phase of current, which

made the time course sigmoidal. (b) The delay at the beginning may reflect a delay in the opening of channels when it has to go through multiple closed states to reach an open state. A conditioning depolarization may help the channel skip the initial several closed states. Therefore, upon further depolarization, the current may develop without delay, and follow a single exponential time course (Byerly et al., 1984). In studying the time course of activation of calcium channels, these two factors should be taken into consideration.

The time courses of the rising phases of type I and type II calcium channel currents are compared in Fig. 3, A and B as they are recorded from a single cell. Type I currents (Fig. 3 A) were obtained by step depolarizations from a holding potential of −70 mV to −40 and −20 mV, at which type II currents were not generated. Type II currents (Fig. 3 B) isolated from the type I component were obtained by step depolarizations from a holding potential of −30 mV to 0 and +20 mV. The amplitudes of depolarizations were the same between the two cases (30 and 50 mV). The time course of activation of type I channels was sigmoidal, whereas that of type II channels appeared to be single exponential rather than sigmoidal. To further analyze the time course of activation, the following method (Okamoto et al., 1976) was used.

By analogy with the Hodgkin-Huxley's formalism for sodium channels (Hodgkin and Huxley, 1952), the time course of a transient inward current, $i(t)$, can be described as $i(t) = Am^x h$, where A is a constant, m is the probability of channel opening, and x is the integer. The activation process is described by a kinetic parameter in the form of m^x. The inactivation process is described using a kinetic parameter, h. These m and h change exponentially with time after a step change of the membrane potential: $m = (m_0 - m_\infty) \exp(-t/\tau_m) + m_\infty$; and $h = (h_0 - h_\infty) \exp \cdot (-t/\tau_h) + h_\infty$, where m_0 and h_0 refer to m and h at time zero, respectively, m_∞ and h_∞ refer to the steady-state values for m and h, respectively, τ_m and τ_h are the time constants of m and h, respectively, and t is the time. For the time after the peak of inward current, i.e., for $t \gg \tau_m$, m can be approximated by m_∞. Therefore, the decay phase of current can be described as $i'(t) = A(m_\infty)^x h$, which represents an exponential decay with a steady-state component. By extrapolation, $i'(t)$ values for the times earlier than the peak ($0 < t < \tau_m$) can be obtained. To analyze the time course of current activation, the membrane is usually stepped from a potential more negative than the channel's activation level. Therefore, m_0 can be regarded as zero. Under such conditions, the ratio of $i(t)$ to $i'(t)$ for a given time before the peak current would yield a relation: $i(t)/i'(t) = [1 - \exp(-t/\tau_m)]^x$; or $1 - [i(t)/i'(t)]^{1/x} = \exp \cdot (-t/\tau_m)$. When the value $1 - [i(t)/i'(t)]^{1/x}$ is plotted against time on a semi-logarithmic scale, it should fall on a straight line if an appropriate integer value, x, is given.

The results of such calculations are shown in Fig. 3, C and D in which the value $1 - [i(t)/i'(t)]^{1/x}$ is plotted

FIGURE 3 Time courses of activation of the two types of calcium channels. (*A*) Transient currents associated with a step depolarization from a holding potential of −70 mV to −40 to −20 mV. (*B*) Long-lasting currents associated with a step depolarization from a holding potential of −30 mV to 0 or +20 mV. Leakage currents have been subtracted. (*C*) Values of ordinate $1 - [i(t)/i'(t)]^{1/x}$, calculated from the current trace of −20 mV shown in *A* are plotted against the time with different values of *x*. (*D*). The same as *C* but at +20 mV shown in *B*. See text for further explanation. Room temperature. Cell, number 28.

against the time. For type I channels (Fig. 3 *C*), the best fit to a straight line was obtained when $x = 2$. A significant deviation from the linearity occurred when $x = 1$ or 3. The data indicated that the activation process of the type I channel had a sigmoidal time course which could be expressed in the form of m^2. A positive shift in the holding potential up to −50 mV did not change the situation (not shown). For type II channels, the best fit to a straight line was obtained with $x = 1$. This indicated that the activation process of type II channels was single exponential, and could be expressed in the form of m^1. However, m^2 may also be the case for type II channels, if a large hyperpolarization was applied prior to the test pulse. This possibility could not be examined because the prepulse to potentials more negative than −30 mV caused a contamination of type I currents.

It should be noted that the slopes of curves in Fig. 3, *C* and *D* are constant, except for the initial phase, regardless of the value of *x* chosen. This indicates that in the equation, $\exp(-t/\tau_m) = 1 - [i(t)/i'(t)]^{1/x}$, the linearity in the semi-logarithmic plot is critical in determining *x*, whereas *x* is not a crucial factor in determining τ_m.

Time Constant of Activation. The time constant of activation, τ_m, was measured for type I and type II currents according to the equation, $\exp(-t/\tau_m) = 1 - [i(t)/i'(t)]^{1/x}$, where $x = 2$ for type I, and $x = 1$ for type II. The results are shown in Fig. 5 (*solid squares* for type I, *open squares* for type II). The value for τ_m of type I channels reached a maximum at −45 mV, which was close to the critical activation level of −50 mV for type I channels. For type II channels, τ_m showed a similar peak, but a much more positive potential (+5 mV) than its critical activation level of −20 mV.

The time constants of activation for potentials more negative than the critical activation level were obtained from the tail current upon repolarization. For type I channels, the maximal transient inward current was induced at −20 mV, and repolarizing pulses to various potentials were applied when the inward current was at the peak (Fig. 4 *A*). For type II channels, the maximal current was induced at +20 mV after the type I component had been inactivated with a holding potential −30 mV. Repolarizing pulses to various potentials were applied 50 ms after the onset of the pulse to +20 mV (Fig. 4 *B*). The tail current decayed with a single exponential time course in either type I or type II channels (Fig. 4, *C* and *D*). The values of τ_m measured on the tail currents are shown in Fig. 5 (*lower half, solid triangles* for type I, *open triangles* for type II).

The results indicated that the potential dependence of the time constant of activation of type II channels measured in the deactivation process was shifted approximately 60 mV in the positive direction from that of type I channels. When compared for the activation process, the shift was reduced to ~30 mV at the most positive potentials measured. The data could be interpreted as indicating that the deactivation rate of type II channels was significantly higher than that of type I channels, whereas the activation rate was similar to each other, if the 30 mV shift in the steady-state kinetics was taken into account.

Rate Constants of Activation. To determine the forward (or activation) and the backward (or deactivation) rate constants, a first-order kinetic model was applied as a first approximation of the activation process of calcium channels. The following relations were used to calculate these rate constants: $k_f = m_\infty/\tau_m$, and $k_b = (1 - m_\infty)/\tau_m$,
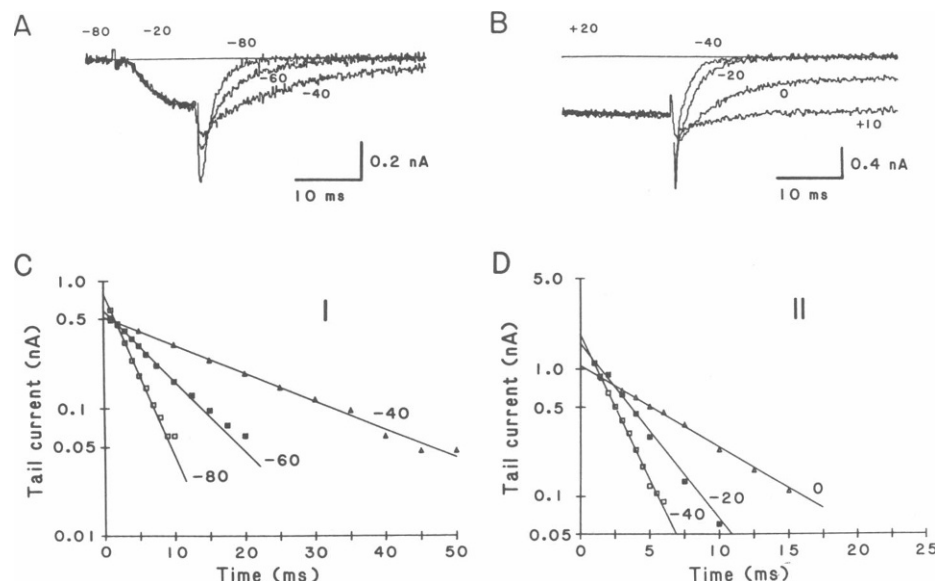
where k_f and k_b are the forward and backward rate constants, respectively. The rate constants thus obtained are shown in Fig. 6, in which the data are plotted against the membrane potential on a semi-logarithmic scale.

The forward rate constants of type I and type II channels both increased in parallel as the membrane was depolarized (slope: 10 mV/e-fold change in the rate constant). The potential dependence of type II channels was shifted ~30 mV in the positive direction from that of type I channels. This 30 mV shift in the forward rate constant

was the same in magnitude as the shifts observed in the steady-state activation and inactivation processes. The backward rate constants of type I and type II channels are shown in Fig. 6 *B*. They both increased in parallel as the membrane was hyperpolarized (slope: 34 mV/e-fold change in the rate constant). The potential-dependent backward rate constant of type II channels was shifted ~60 mV in the positive direction from that of type I channels. This shift was consistent with the shift in the time constant of the deactivation process (Fig. 5). The data indicated that the backward rate constant of type II channels was 2.4 times larger than that of type I channels if compared at potentials 30 mV more positive for type II channels.

Time Course of Inactivation. The presence of the fast inactivation characterizes type I channels. However, a very slow inactivation occurs in both type I and type II channels (see Fig. 3, *A* and *B*, in Narahashi et al., 1987). We have measured the time constant of the fast inactivation (τ_h) of type I channels to compare it with τ_m. For potentials more positive than the critical activation level of −50 mV, τ_h was measured directly on the current traces, assuming that the slow component was constant. For potentials more negative than −50 mV, τ_h was measured on the recovery from inactivation during a repolarization, using the conventional double pulse protocol. The results are shown in Fig. 5 (*upper portion*). The value for τ_h showed a peak at −55 mV, and was one order of magnitude greater than τ_m for potentials more negative than −40 mV. This suggested that the deactivation process of type I channels, observed at these potentials, was not affected by a recovery from the inactivation that might have developed during a test pulse.

We did not examine the slow component of inactivation of type I channels, or the slow inactivation of type II channels. It remains to be seen whether the time constants
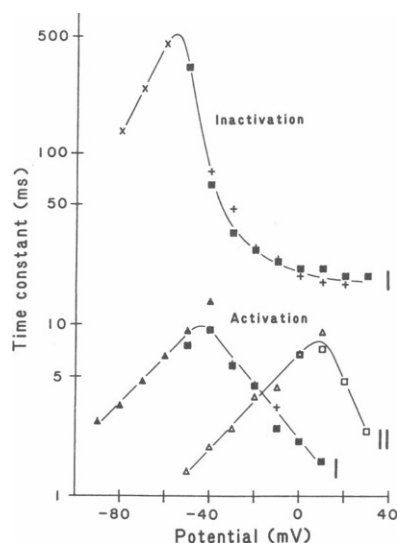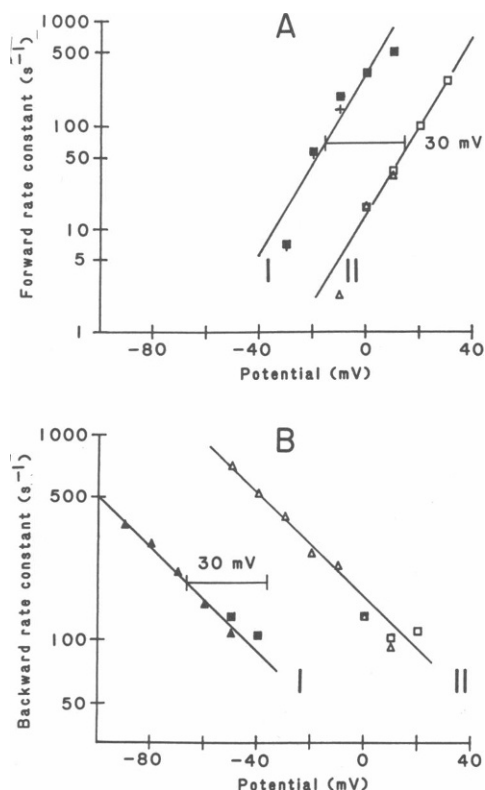

FIGURE 5 Time constants of activation and inactivation of the two types of calcium channels as a function of the membrane potential. *Bottom*, time constants of activation for the current activation (*squares* and +) and deactivation (*triangles*). Filled symbols and + are for type I. Open symbols are for type II. *Top*, time constants of inactivation of type I channels for the current decay (■,+) and for the recovery from inactivation (×). Solid curves are drawn by eye. Room temperature. Cells: number 19 (■,△), number 28 (□,△,+), number 31 (×).

FIGURE 6 Forward (*A*) and backward (*B*) rate constants for activation as a function of the membrane potential. Filled symbols and + are for type I. Open symbols are for type II. The same data and symbols as those in Fig. 5. Steady-state activation levels used in calculating the rate constants were obtained from Fig. 2 *A*.

of the slow inactivation of the two channel types show a potential shift of 30 mV as has been seen in other gating kinetics.

II. Permeation Properties

Calcium channels are mainly permeable to the divalent cations Ca^{2+}, Sr^{2+}, and Ba^{2+}. Other divalent cations are not only impermeant, but also often show blocking effects on the passage of permeant cations. The sequence of permeability among Ca^{2+}, Sr^{2+}, and Ba^{2+}, as well as the sequence of blocking effects of other divalent cations, differ significantly among calcium channels examined in different tissues (see Hagiwara and Byerly, 1981). In the neuroblastoma cell, it was shown that type II calcium

channels were preferentially blocked by a low concentration of Cd^{2+} (Narahashi et al., 1987).

Ion Selectivity among Ca^{2+}, Sr^{2+}, and Ba^{2+} Ions. Fig. 7 shows Ba^{2+}, Ca^{2+}, and Sr^{2+} currents through type I calcium channels (*upper traces*) and those through type II channels (*lower traces*) as recorded from a single cell. Ca^{2+} and Sr^{2+} currents were obtained by replacing Ba^{2+} (50 mM) in the external solution with equimolar Ca^{2+} and Sr^{2+}, respectively. Transient Ba^{2+}, Ca^{2+}, and Sr^{2+} currents were obtained at −20 mV, and their time courses and amplitudes are compared in Fig. 7, *upper traces*. The Ca^{2+} and Sr^{2+} currents showed activation-inactivation time courses similar to those of the Ba^{2+} current. The amplitudes of the Ba^{2+} and Sr^{2+} currents were almost identical, whereas that of the Ca^{2+} current was smaller. This suggested that the selectivity of type I calcium channels was in the sequence of $Ba^{2+} = Sr^{2+} > Ca^{2+}$. Fig. 8 *A* shows their I-V relationships for the peak amplitude of the inward current. From the I-V relations, the maximum amplitude of the inward current was measured for each ion to determine the relative permeability. The permeability thus determined was as follows: $P_{Ba}/P_{Sr}/P_{Ca} = 1.0:1.0:0.7$ (type I channels).

Ba^{2+}, Ca^{2+}, and Sr^{2+} also caused long-lasting inward currents (Fig. 7, *lower traces*). However, the potential at which a maximal inward current was induced was different among the divalent cations; +20 mV for Ca^{2+} and +10 mV for Ba^{2+} and Sr^{2+}. Therefore, to compare the current amplitudes, Ba^{2+} and Sr^{2+} currents were obtained at +10 mV, and Ca^{2+} current was obtained at +20 mV. A conditioning depolarization was not applied to inactivate the type I component, because this component was expected to be fully inactivated at the end of the 160-ms test pulse as has been shown previously (Narahashi et al., 1987). Therefore, the current amplitude at 160 ms represents the amplitude of the type II current. As can be seen in Fig. 7 (*lower traces*), the Sr^{2+} current was smaller than the Ba^{2+} current, and the Ca^{2+} current was much smaller than any of them. This suggested that the selectivity of type II channels was in the sequence of $Ba^{2+} > Sr^{2+} \gg Ca^{2+}$. Fig. 8 *B* shows their I-V relationships as measured at 160 ms after beginning of the pulse. The relative permeability was obtained from the maximum amplitude for each ion. The permeability ratio for type II calcium channels thus determined was: $P_{Ba}/P_{Sr}/P_{Ca} = 1.0:0.7:0.3$.
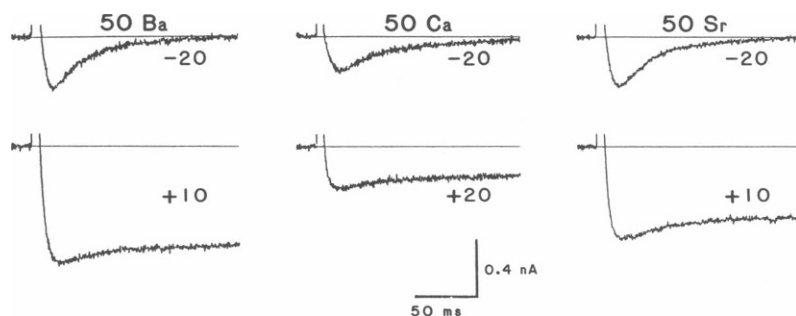

FIGURE 7 Comparison of the two components of Ba^{2+} current with those of Ca^{2+} and Sr^{2+} currents in calcium channels. All current traces were obtained from a single cell. Leakage currents have been subtracted. Holding potential, −80 mV. 50 mM Ba^{2+} in the external solution was replaced with Ca^{2+}, then Sr^{2+}, and back to Ba^{2+}. Current traces in recovery (not shown) were practically identical to the control records. Room temperature. Cell, number 13.
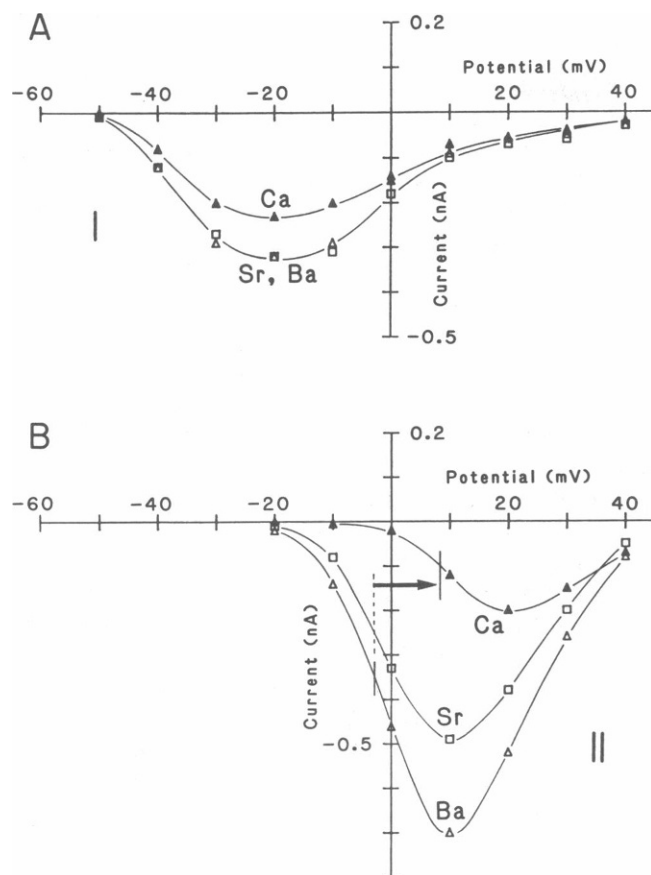
FIGURE 8 Current-voltage relations for Ca^{2+}, Sr^{2+}, and Ba^{2+} currents through type I (A) and type II (B) calcium channels. The current amplitudes were measured at the peak of the transient current (A) or at the end of a 160-ms voltage pulse (B). In addition to the linear leakage subtractoin, an outward current component determined after blocking the calcium channels with 1 mM La^{3+} was also subtracted. The vertical bars in B indicate the potentials at which inward currents attain their half-maximal amplitudes. The same cell as that in Fig. 7.

Ion Selectivity Corrected for Surface Charge Effect. The I-V relationship for the Ca^{2+} current through type II calcium channels is located 10–12 mV more positive than that of the Ba^{2+} current (Fig. 8 B, arrow). In the I-V relationships for type I channels, however, no obvious potential shift was observed (Fig. 8 A). Such a shift in the I-V relationship in the positive direction along the voltage axis has been attributed to a positive shift in the surface potential due to neutralization of negative surface charges by Ca^{2+} (Frankenhaeuser and Hodgkin, 1957; Gilbert and Ehrenstein, 1969). The data suggested that there were surface charges around type II channels, but not around type I channels.

According to Ohmori and Yoshii (1977), negative surface charges can attract permeant cations and increase their concentration at the surface according to the Boltzmann distribution as a function of the surface potential. If certain cations such as Ca^{2+} capable of binding to the negative charges are present, the negative surface potential will be decreased through neutralization of the charges (or

shift to the positive potential). Therefore, the permeant cations attracted to the surface and available for calcium channels will be decreased, thus leading to a decrease in the inward current carried by the permeant cations. Based on their theory, the ratio of Ca^{2+} permeability to Ba^{2+} permeability determined by the maximum current amplitude can be corrected for the surface concentrations of these cations by the relation:

$$P_{Ca}^{*}/P_{Ba}^{*} = (I_{Ca}/I_{Ba}) \exp (\Delta V_{s} 2F/RT),$$

where P_{Ca}^{*} and P_{Ba}^{*} are corrected permeabilities for Ca^{2+} and Ba^{2+}, respectively; I_{Ca} and I_{Ba} are Ca^{2+} and Ba^{2+} currents, respectively, at a given transmembrane potential corrected for the surface potential; ΔV_{s} represents a shift in the surface potential; and F/RT has the usual thermodynamic meanings. For calcium channels, the ratio between two maximum inward currents of different divalent cations, X and Y, gives a good approximation of P_{X}/P_{Y}, and a voltage shift in the I-V relations, as measured at a half-maximal amplitude of current, gives a value of ΔV_{s} (Ohmori and Yoshii, 1977). Therefore, by applying values of $I_{Ca}/I_{Ba} = P_{Ca}/P_{Ba} = 0.3$, and $\Delta V_{s} = 10$–12 mV to the equation, the corrected permeability ratio was calculated as $P_{Ca}^{*}/P_{Ba}^{*} = 0.66$–0.77 (at 22°C). This corrected permeability ratio for type II channels is consistent with the uncorrected permeability ratio for type I channels, i.e., $P_{Ca}/P_{Ba} = 0.7$.

The low permeability ratio, $P_{Sr} = P_{Ba} = 0.7$, of type II channels as compared with the ratio of type I channels ($P_{Sr}/P_{Ba} = 1.0$) might also be due to a binding effect of Sr^{2+} to the surface charges near type II channels. To explain this reduction, only +4.5 mV shift in the surface potential is necessary. However, it was difficult to determine from the I-V curves of type II channels whether a 5 mV positive shift occurred from Ba^{2+} to Sr^{2+}. The results suggested that the ion permeation mechanisms between two types of calcium channels were similar to each other, despite the differences in apparent permeability ratios among divalent cations.

DISCUSSION

The present study has shown that two types of calcium channels in neuroblastoma cells have many properties in common with respect to their gating and ion permeation mechanisms despite their apparent differences in the membrane potential dependence and ion selectivity. Apart from the absence of fast inactivation, the major factors that differentiate type II channels from type I were relative in nature, such as a positive shift in the potential dependence and a higher density of surface charges. In addition, the turn-off kinetics of the activation of type II channels were 2.4 times faster than those of type I channels.

Steady-state Activation and Inactivation

Both steady-state activation and inactivation curves for type II calcium channels were shifted ~30 mV in the

892

positive direction from those of type I channels. To our knowledge, this is the first report which indicates that two coexisting types of calcium channels have the identical steady-state gating characteristics with only the membrane potential dependence shifted. There are two possible explanations for such a potential shift: a different voltage sensor of the gating machinery or a different effective membrane potential. Since the sensitivities of the gatings to the potential, represented by the slopes of the steady-state activation and inactivation curves, were identical in both types of calcium channels, it was assumed that the voltage sensor of each gating is the same. Therefore, the effective electric field seen by the voltage sensor of the gating machinery would be different between the two types. It was further assumed that the surface negative charges, which have been suggested to be present near type II calcium channels but not type I channels (Bean, 1985), are, at least in part, responsible for creating the difference in the effective transmembrane potential.

Two types of calcium channels identified in other preparations such as pituitary tumor cells (Armstrong and Matteson, 1985) and sensory neurons (Fedulova et al., 1985) also show a similar difference in the critical activation levels, but with a smaller shift of 20 mV as against 30 mV for neuroblastoma cells. This might be related to the difference in the concentration of divalent cations in salines: 50 mM Ba^{2+} in our case and 10–15 mM Ca^{2+} in others. Saline solution with 50 mM Ba^{2+} may be more effective than that with 10–15 mM Ca^{2+} in causing a positive voltage shift in the current-voltage relation for type II channels. Such a larger difference in voltage dependence of gating between type I and type II calcium channels was helpful in separating the type II current from the type I component as described previously (Narahashi et al., 1987).

Activation Kinetics

By analogy with sodium and potassium channels, the Hodgkin-Huxley kinetic parameters (Hodgkin and Huxley, 1952) have been used for calcium channels to describe the time course of activation and inactivation (Okamoto et al., 1976; Kostyuk et al., 1977; Akaike et al., 1978). We have also used this formalism for type I calcium channels to isolate the activation process from the contamination of the fast inactivation and for both types of channels to compare the activation kinetics. The time courses of the activation of type I and II currents are best described in the form of m^2 and m^1, respectively, in which m refers to a dimensionless parameter for activation which varies with membrane potential and time. However, in calculating the forward and backward rate constants of activation which can be derived form the time constant of $m(\tau_m)$ and the steady-state value of $m(m_\infty)$, we used the apparent steady-state activation levels as shown in Fig. 2 A as a measure of m_∞ without correction for the power of m. Therefore, the rate constants obtained represent the apparent values such as those described in a two-state model for channel opening and closing. The reasons for this simplification are as follows.

(a) Recent single channel studies of calcium channels have shown that the Hodgkin-Huxley model does not describe the channel events. Rather a sequential model with multiple closed states and an open state predicts the events better (Fenwick et al., 1982; Reuter et al., 1982; Hagiwara and Ohmori, 1983; Brown et al., 1984). (b) A conditioning depolarization may alter the time course of the current from the one described by m^2 to that predicted by m^1 (Byerly et al., 1984). This indicates that the correction of m according to the power of m is meaningless. Therefore, (c) apparent rate constants would be more appropriate to represent unknown rate limiting steps of the activation gate and to compare them between the two channel types.

The forward rate constants for activation of type I and type II calcium channels were both voltage-dependent, but the curves relating the rate constant to membrane potential are separated by 30 mV between the two types. The curves relating the backward rate constant, which represents the turn-off process upon repolarization, to membrane potential were also voltage-dependent but separated by as much as 60 mV between the two types. Based on the assumption that the effective transmembrane potential for the type II channel gating is 30 mV more positive than that for the type I, it was concluded that the turn-off of the type II current was 2.4 times faster than that of the type I current. If compared at the same membrane potential in the absolute scale, the difference is magnified to about 7 times. This predicts that a tail current of mixed current components comprises a very fast and slow component. In pituitary cells, Armstrong and Matteson (1985) have observed such fast and slow components of tail currents through two different types of calcium channels which correspond to the type II and type I channels, respectively.

The sequential model for the single channel behavior of calcium channels also predicts fast and slow turn-off processes. Fast and slow Ca^{2+} tail currents in snail neurons have been analyzed based on this prediction (Byerly et al., 1984). However, it was not clear whether these two components originated from a single type of calcium channels or from two different types of calcium channels (see also Brown et al., 1981). It remains to be seen whether the tail current of each channel type in neuroblastoma cells comprises two components as predicted. With a limited time resolution in the present study (0.5–1.0 ms at best), a fast component may have been missed.

Inactivation Kinetics

A variety of mechanisms of calcium channel inactivation has been found: A voltage-dependent fast inactivation, a Ca^{2+}-mediated inactivation, and a very slow inactivation (see Hagiwara and Byerly, 1981; Tsien, 1983; Eckert and

Chad, 1984). In the present study, Ba^{2+} currents through type I channels were inactivated promptly but those through type II channels were inactivated very slowly. The inactivation of type I calcium channels changed with membrane potential. This could be due to membrane current rather than membrane potential, but the possibility can be excluded for the following reasons.

(a) The time constant of the current decay (τ_h) decreased with depolarization in the membrane potentials ranging from -60 to $+30$ mV, whereas the peak inward current reached its maximum amplitude at -20 mV and decreased with either depolarization or hyperpolarization (Figs. 5 and 8 A). (b) Sr^{2+} and Ba^{2+} currents decayed at the same rate as Ca^{2+} current (Fig. 7, upper traces). In Ca^{2+}-mediated inactivation, Ca^{2+} current decays more rapidly than Ba^{2+} current (see Eckert and Chad, 1984). (c) More than 50% steady-state inactivation was observed at -50 mV which was the critical activation potential for type I channels (Fig. 2). All of these observations are not consistent with the current-dependent inactivation.

Calcium channels showing a fast voltage-dependent inactivation have been identified mainly in various egg cells including mouse eggs (see Hagiwara and Jaffe, 1979; Hagiwara and Byerly, 1981). In most mammalian neurons, the major population of calcium channels seems to be type II (see Tsien, 1983). Neuroblastoma cells are exceptional where type I channels are the major component of calcium channels (Moolenaar and Spector, 1978; Fishman and Spector, 1981; Quandt and Narahashi, 1984). Type I channels have also been found in non-neuronal cells such as myeloma cells and B lymphocytes (Fukushima and Hagiwara, 1983, 1985).

Ion Selectivity and Surface Charge Effect

Based on the amplitude of the inward current, relative permeabilities to three divalent cations were estimated to be $Ba^{2+}/Sr^{2+}/Ca^{2+} = 1.0:1.0:0.7$ for type I calcium channels and $1.0:0.7:0.3$, for type II channels. Thus type II channels are selective to these three divalent cations of which Ba^{2+} is most permeant, whereas type I channels are less selective.

These estimates of relative permeabilities were based on the assumption that the probability of channel openings was the same among these permeant cations. The effective transmembrane potential which could be changed by the surface potential was corrected by comparison of the maximum amplitudes of the inward currents as had been done in the other preparations (Ohmori and Yoshii, 1977). Further correction was made for the surface concentration of the permeant cations as a function of the surface potential, which had been shown to affect the conductance in the biological membranes (Ohmori and Yoshii, 1977) as well as in artificial membranes (McLaughlin et al., 1970). With these corrections it was concluded that type II channels were as less selective as type I channels, and that

the surface negative charges around type II channels made Ba^{2+} an effective charge carrier through the channels.

Origin of the Two Types of Calcium Channels

A development study on membrane excitability in ascidian embryos has shown that calcium channels appearing at early stages of development are type I, whereas those developed at later stages are type II (Hirano and Takahashi, 1984). In the present study, we have found that the two types of calcium channels have many properties in common, suggesting that the origins of the two channel types are the same. This supports the idea that the type II calcium channels are derived from the type I calcium channels.

REFERENCES

Akaike, N., K. S. Lee, and A. M. Brown. 1978. The calcium current of Helix neuron. J. Gen. Physiol. 71:509–531.

Armstrong, C. M., and D. R. Matteson. 1985. Two distinct populations of calcium channels in a clonal line of pituitary cells. Science (Wash. DC). 227:65–67.

Bean, B. P. 1985. Two kinds of calcium channels in canine atrial cells. Differences in kinetics, selectivity, and pharmacology. J. Gen. Physiol. 86:1–30.

Brown, A. M., K. Morimoto, Y. Tsuda, and D. L. Wilson. 1981. Calcium current-dependent and voltage-dependent inactivation of calcium channels in Helix aspersa. J. Physiol. (Lond.). 320:193–218.

Brown, A. M., H. D. Lux, and D. L. Wislon. 1984. Activation and inactivation of single calcium channels in snail neurons. J. Gen. Physiol. 83:751–769.

Byerly, L., P. B. Chase, and J. R. Stimers. 1984. Calcium current activation kinetics of neurones of the snail Lymnaea stagnalis. J. Physiol. (Lond.). 348:187–207.

Eckert, R., and J. E. Chad. 1984. Inactivation of Ca channels. Prog. Biophys. Mol. Biol. 44:215–267.

Fedulova, S. A., P. G. Kostyuk, and N. S. Vaselovsky. 1985. Two types of calcium channels in the somatic membrane of new-born rat dorsal root ganglion neurones. J. Physiol. (Lond.). 359:431–446.

Fenwick, E. M., A. Marty, and E. Neher. 1982. Sodium and calcium channels in bovine chromaffin cells. J. Physiol. (Lond.). 331:599–635.

Fishman, M. C., and I. Spector. 1981. Potassium current suppression by quinidine reveals additional calcium currents in neuroblastoma cells. Proc. Natl. Acad. Sci. USA. 78:5245–5249.

Frankenhaeuser, B., and A. L. Hodgkin. 1957. The action of calcium on the electrical properties of squid axons. J. Physiol. (Lond.). 137:218–244.

Fukushima, Y., and S. Hagiwara. 1983. Voltage-gated Ca^{2+} channels in mouse myeloma cells. Proc. Natl. Acad. Sci. USA. 80:2240–2242.

Fukushima,Y., and S. Hagiwara. 1985. Currents carried by monovalent cations through calcium channels in mouse neoplastic B lymphocytes. J. Physiol. (Lond.). 358:255–284.

Gilbert, D. L., and G. Ehrenstein. 1969. Effect of divalent cations on potassium conductance of squid axons: determination of surface charge. Biophys. J. 9:447–463.

Goldman, D. E. 1943. Potential, impedance and rectification in membranes. *J. Gen. Physiol.* 27:37–60.

Hagiwara, S., and L. A. Jaffe. 1979. Electrical properties of egg cell membrane. *Annu. Rev. Biophys. Bioeng.* 8:385–416.

Hagiwara, S., and L. Byerly. 1981. Calcium channel. *Annu. Rev. Neurosci.* 4:69–125.

Hagiwara, S., and H. Ohmori. 1983. Studies of single calcium channel currents in rat clonal pituitary cells. *J. Physiol. (Lond.).* 336:649–661.

Hamill, O. P., A. Marty, E. Neher, B. Sakmann, and F. J. Sigworth. 1981. Improved patch-clamp techniques for high-resolution current recording from cells and cell-free membrane patches. *Pfluegers Arch.* 391:85–100.

Hille, B. 1967. The selective inhibition of delayed potassium currents in nerve by tetraethylammonium ion. *J. Gen. Physiol.* 50:1287–1302.

Hirano, T., and K. Takahashi. 1984. Comparison of properties of calcium channels between the differentiated 1-cell embryo and the egg cell of ascidians. *J. Physiol. (Lond.).* 347:327–344.

Hodgkin, A. L., and B. Katz. 1949. The effect of sodium ions on the electrical activity of the giant axon of the squid. *J. Physiol. (Lond.).* 108:37–77.

Hodgkin, A. L., and A. F. Huxley. 1952. A quantitative description of membrane current and its application to conduction and excitation in nerve. *J. Physiol. (Lond.).* 117:500–544.

Kimhi, Y., C. Palfrey, I. Spector, Y. Barak, and U. Z. Littauer. 1976. Maturation of neuroblastoma cells in the presence of dimethylsulfoxide. *Proc. Natl. Acad. Sci. USA.* 73:462–466.

Kostyuk, P. G., O. A. Krishtal, and Y. A. Shakhovalov. 1977. Separation of sodium and calcium currents in the somatic membrane of mollusc neurones. *J. Physiol. (Lond.).* 270:545–568.

McLaughlin, S. G. A., G. Szabo, G. Eisenman, and S. M. Ciani. 1970. Surface charge and the conductance of phospholipid membranes. *Proc. Natl. Acad. Sci. USA.* 67:1268–1275.

Moolenaar, W. H., and I. Spector. 1978. Ionic currents in cultured mouse neuroblastoma cells under voltage-clamp conditions. *J. Physiol. (Lond.).* 278:265–286.

Narahashi, T., J. W. Moore, and W. R. Scott. 1964. Tetrodotoxin blockage of sodium conductance increase in lobster giant axons. *J. Gen. Physiol.* 47:965–974.

Narahashi, T., A. Tsunoo, and M. Yoshii. 1987. Characterization of two types of calcium channels in mouse neuroblastoma cells. *J. Physiol. (Lond.).* 383:231–249.

Ohmori, H., and M. Yoshii. 1977. Surface potential reflected in both gating and permeation mechanisms of sodium and calcium channels of the tunicate egg cell membrane. *J. Physiol. (Lond.).* 267:429–463.

Okamoto, H., K. Takahashi, and M. Yoshii. 1976. Two components of the calcium current in the egg cell membrane of the tunicate. *J. Physiol. (Lond.).* 255:527–561.

Quandt, F. N., and T. Narahashi. 1984. Isolation and kinetic analysis of inward currents in neuroblastoma cells. *Neuroscience.* 13:249–262.

Reuter, H., C. F. Stevens, R. W. Tsien, and G. Yellen. 1982. Properties of single calcium channels in cardiac cell culture. *Nature (Lond.).* 297:501–504.

Tsien, R. W. 1983. Calcium channels in excitable cell membranes. *Annu. Rev. Physiol.* 45:341–358.

Tsunoo, A., M. Yoshii, and T. Narahashi. 1984. Two types of calcium channels in neuroblastoma cells and their sensitivities to cyclic AMP. *Soc. Neurosci. Abstr.* 10:527.

Tsunoo, A., M. Yoshii, and T. Narahashi. 1986. Block of calcium channels by enkephalin and somatostatin in neuroblastoma-glioma hybrid NG108-15 cells. *Proc. Natl. Acad. Sci. USA.* 83:9832–9836.

Yoshii, M., A. Tsunoo, and T. Narahashi. 1985. Different properties in two types of calcium channels in neuroblastoma cells. *Biophys. J.* 47:433a (Abstr.).